

Electronic excited states at ultrathin dielectric-metal interfacesL. Sementa,¹ A. Marini,² G. Barcaro,¹ F. R. Negreiros,¹ and A. Fortunelli^{1,*}¹*CNR-IPCF, Consiglio Nazionale delle Ricerche, v. G. Moruzzi 1, Pisa, Italy*²*CNR-ISM, Consiglio Nazionale delle Ricerche, v. Salaria Km 29.5, Monterotondo, Italy*

(Received 10 April 2013; revised manuscript received 6 June 2013; published 9 September 2013)

Electronic excited states at a bcc(110) lithium surface, both bare and covered by ionic ultrathin (1–2 monolayers) LiF epitaxial films, are investigated via many-body perturbation theory calculations achieving an atomistic level of detail. The full self-consistent solution of the GW equations is used to account for correlation effects and to properly describe the screened potential in the vacuum. In addition to the correct prediction of image-potential states, we find that the mixing between resonances and image states and the charge compression due to the dielectric ultrathin overlayer give rise to excitations with a hybrid localized but low-lying character whose accurate description cannot intrinsically be achieved via simple models or low-level calculations, but which are expected to play a crucial role in determining the electronic response and transport properties of these systems.

DOI: [10.1103/PhysRevB.88.125413](https://doi.org/10.1103/PhysRevB.88.125413)

PACS number(s): 73.20.At, 73.21.Ac, 73.40.–c, 77.55.–g

Dielectric ultrathin films are of great interest in several fields, ranging from nanoelectronics to chemistry, at both fundamental and applied levels.^{1–3} Nanometer thickness endows them with a conductive character—at variance with their bulk form—and thus the possibility to mediate and tune electron transport processes between the underlying metal substrate and the exterior, such as adsorbates⁴ or conducting tips,⁵ giving rise to peculiar chemical and physical phenomena. Electronic excited states at the dielectric-metal interface play a crucial role in such processes, whence the rapidly increasing attention devoted to them in recent years at both the experimental and theoretical levels.^{6–8} Roughly speaking, excited states at surfaces can be classified either as resonances or image states. Resonances are virtual or unoccupied levels lying close to the Fermi energy which are strongly localized on the outermost interfacial layers of the system. Image states are quantized electronic states that exist in principle at any surfaces (in particular metal ones) with a band gap near the vacuum level. The Coulomb-like attractive image forces, experienced by any charged particle in front of a conductive material,⁹ or dielectric polarization forces,¹⁰ together with the repulsion due to the electronic clouds of the surface atoms, form a potential well for weakly bound electrons, whose energy levels are described by a hydrogenic Rydberg series. Even though their basic physics is qualitatively understood, there is a lack of first-principles accurate theoretical predictions on such states, especially for nonstandard surfaces or when the metal surface is covered with, e.g., an ultrathin layer of an ionic compound.^{1–3} Producing rigorous information on this topic is thus a necessary step to make further progress in the field.

In the present work we tackle such a problem, and investigate via many-body perturbation theory (MBPT) the lowest electronic excited states of a simple metal surface both bare and covered by a dielectric ultrathin [1–2 monolayers (MLs)] film. We use MBPT not simply as an *a posteriori* correction, but in a computationally demanding, fully self-consistent fashion which is the mandatory level of theory to achieve a proper description of the screened potential in vacuum.^{9,11} In addition to the correct prediction of several image states, we find that surface resonances are present, and that the coupling between resonances and image states as a

function of the compression effect due to the dielectric ultrathin overlayer gives rise to excitations lying close to the Fermi energy but with no major components on the outermost surface atomic layers. An accurate description of these excitations cannot intrinsically be achieved via simple models or low-level calculations, but they are expected to play a crucial role in emerging phenomena such as electronically induced adsorbate reactions or quantum conductance. As we argue below, the interference between surface resonances and image states can also strongly perturb the hydrogenic series of the latter and hinder parametric analyses: This explains why the correct assignment and understanding of electronic excited states at metal-dielectric interfaces can be uncertain and a matter of controversy even at a qualitative level,¹² and why estimates of physical quantities extracted by fitting scanning tunneling spectroscopy (STS) resonances can be in disagreement with those derived via different experimental techniques.⁶

We choose a simple metal surface covered with an ionic dielectric as a prototypical system to explore and test the approach: the bcc(110) lithium surface, both bare and covered by lithium fluoride (LiF) monolayer (ML) and bilayer (BL) films. Figure 1 shows a pictorial image of the investigated geometries (more details can be found in the Supplemental Material¹³).

All calculations are performed using the ABINIT code¹⁴ employing plane-wave basis sets and norm-conserving pseudopotential obtained using the Troullier-Martin scheme.¹⁵ The Kohn-Sham equations are solved using the local density approximation (LDA) for the exchange-correlation functional; see the Supplemental Material¹³ for further information. Even though the basic physics of surface resonances and image-potential states is qualitatively understood, the predictive description of such states is quite difficult. Surface resonances cannot be described via model (e.g., jellium) calculations¹⁶ but require an atomistic level of detail.⁷ For image states, mean-field approaches (including density-functional theory, DFT) do not predict the correct spatial Coulombic decay of the potential outside the surface for unoccupied levels^{9,17} and one has to resort to computationally demanding many-body perturbation theory (MBPT) or post-DFT methods¹⁸ even for a qualitative description of these states. While this

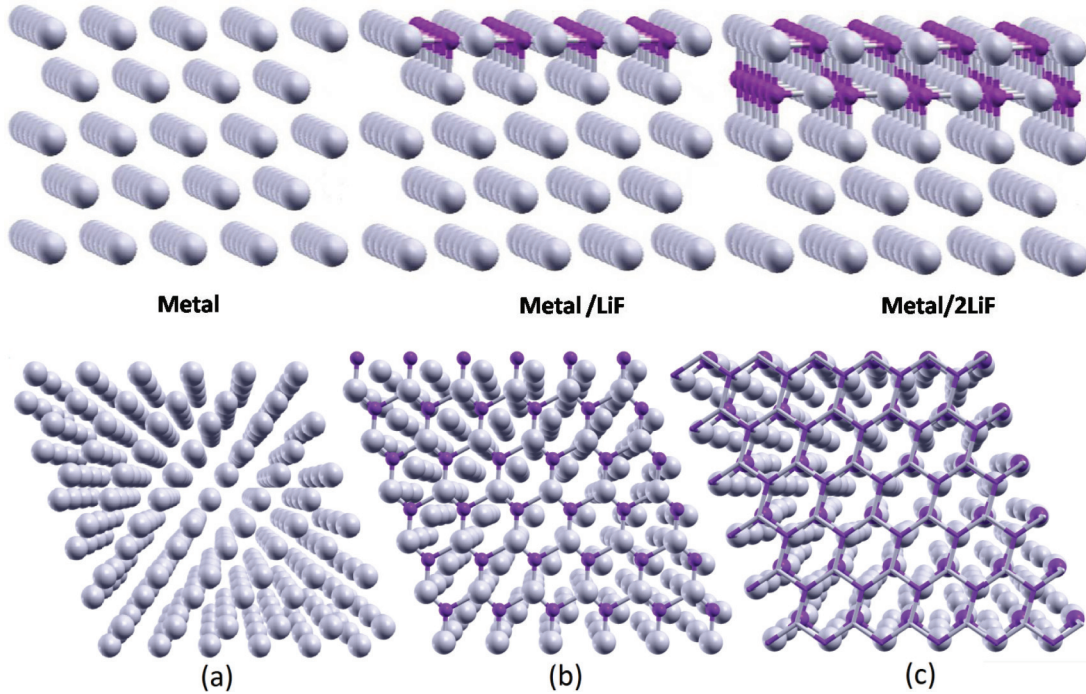


FIG. 1. (Color online) Pictorial views of the systems here investigated: a Li(100) slab [metal] (a) covered with a ML [metal/LiF] (b) or a BL [metal/2LiF] (c) film of LiF. The top row (with only the five topmost layers) shows a side view, the bottom row, a top view. Li in light shade (gray), F in dark shade (magenta).

can be bypassed for known and well-characterized surfaces by referring to experiment—whence one derives effective parameters to empirically correct the out-of-the-surface tail of the mean-field potential on which the electron dynamics occur¹⁹—the situation for nonstandard surfaces or when the metal surface is covered with, e.g., an ultrathin layer of an ionic compound² is completely unknown.

MBPT-based methods¹⁸ represent an approach for obtaining quasiparticle (QP) levels in a controlled manner that is amenable to systematic improvements. This makes this approach tractable for the large systems needed to simulate defects and interfaces.²⁰ Here, the many-electron problem is treated via the self-consistent solution of the Dyson equation in the so-called GW approximation.²¹ This self-consistent solution corresponds to a modified mean-field problem for the electrons where the DFT potential is replaced by a spatially nonlocal self-energy operator evaluated within the GW approximation. In particular, the quasiparticle self-consistent GW approach (QSGW) of Faleev *et al.*²² is used which allows us to go beyond the first-order perturbation to the LDA and calculate quasiparticle (QP) wave functions. In Faleev's approximation to the GW equations²³ a static and Hermitian self-energy reduces the computational costs at the price of losing information on the lifetime of the quasiparticles. Within the GW scheme, the bare Coulomb interaction is renormalized by the electronic screening, which, in turn, is calculated using the dielectric response function $\epsilon(\mathbf{q}, \omega)$. This latter function is approximated by employing the LDA wave functions and a plane-wave expansion cutoff of 5.0 a.u. As a full energy-dependent description of the screened interaction is computationally demanding, we resort to the Godby-Needs plasmon-pole approximation (PPA) to describe its dynamical

behavior²⁴ which is interpolated on the basis of an explicit calculation of $\epsilon(\mathbf{q}, \omega)$ at two frequencies: $\omega_1 = 0$ and ω_2 . In our calculations we choose a value for the plasma-frequency ω_2 parameter equal to 8.30 eV, which corresponds to the plasmon resonance of bulk lithium. We denote by the acronym sc-PPA the results of the self-consistent PPA calculations. More details are given in the Supplemental Material.¹³

On the bare Li(110) surface there are no occupied surface states but the first excited state above the Fermi level is a resonance, as can be seen in Fig. 2 where its form and localization on the topmost layers can be appreciated. At higher energies several image states appear. From Fig. 2, where a comparison of LDA and sc-PPA wave function profiles is shown, one sees that both the resonance and the first imagelike virtual state are reasonably well predicted already at the LDA level. The reason for this lies in the extension of the tail of the LDA potential outside the surface: As shown in Fig. S5 of the Supplemental Material,¹³ this tail is attractive enough to support localized states. The self-consistent GW does not drastically change this form, in keeping with previous work.⁹ The effect of correlation is instead apparent in the third excited state, which at the LDA level has basically the shape of a particle-in-the-box wave function whereas at the sc-PPA level it shrinks and approaches the surface correctly assuming the form of a second image state (see Fig. 2). The energy values reported in Table I compare well with experiment: For example, the difference between the first two image states is 0.55 eV from sc-PPA and 0.53 eV from experiment,¹⁹ and they are in fair agreement with previous studies, except for the resonance state, which lies at higher energy from our calculations (no experimental data are available which could validate one approach). For the sake of completeness, we also

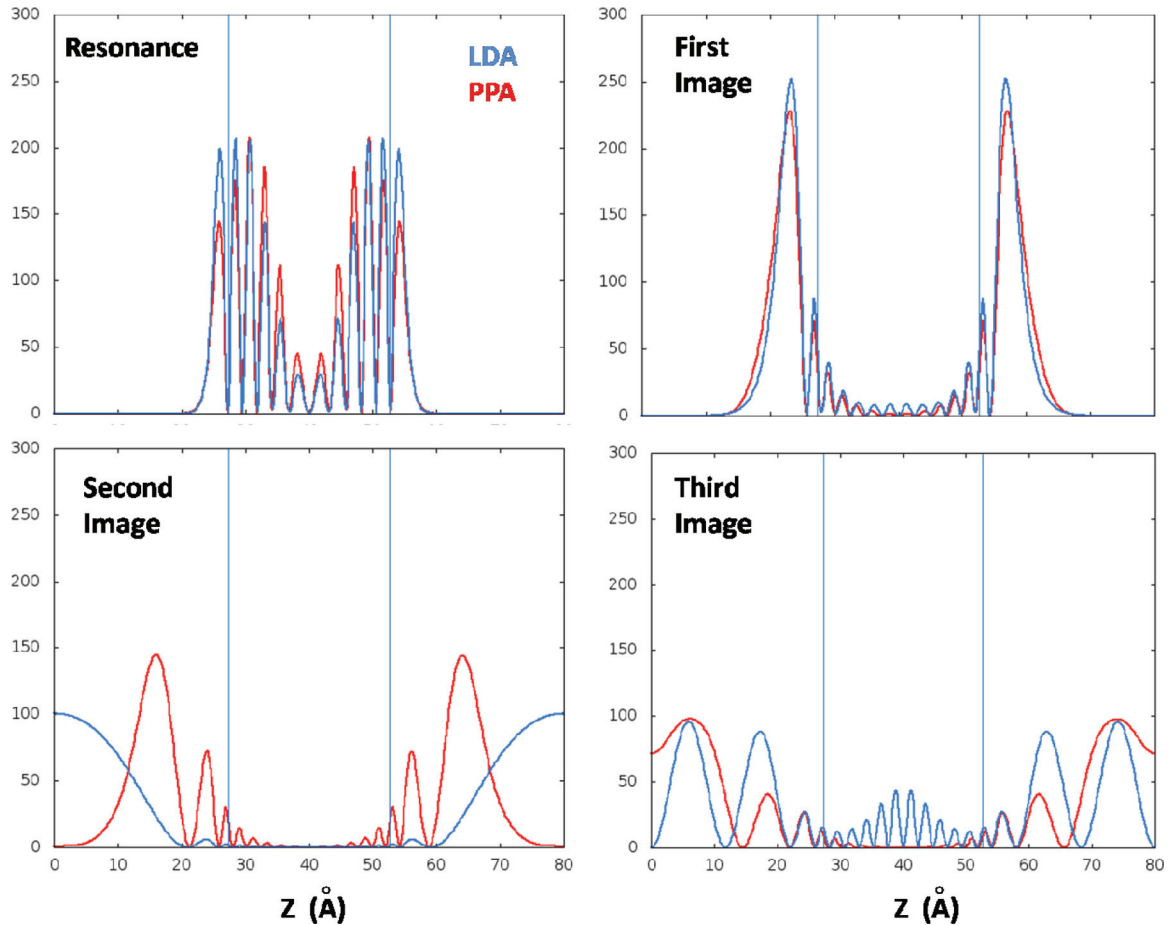


FIG. 2. (Color online) One-dimensional profiles along the z direction obtained by averaging over (x,y) planes the square modulus of the wave function for several excited states of Li(110) at the LDA [light gray (blue)] and QSGW-PPA [dark gray (red)] level. “Resonance” is the surface resonance state, “First Image” the first image (second excited) state, etc. Z values in Å. The vertical lines indicate the position of the outmost surface layers.

report in Fig. 2 what can be considered at the sc-PPA level as the third image state (a successive particle-in-the-box state at the LDA level), which however—due to the limited size of the unit cell in the z direction—overlaps with its replicated image and is thus appreciably deformed.

When one LiF ML is adsorbed on the Li(110) surface, a noteworthy effect can be observed (see Fig. 3): At the LDA level the first excited state has the mixed features of a combination of an image state and a bulk state, but these features disappear at the sc-PPA level producing a wave function localized in close proximity of the surface (even closer than the first image state on the bare Li surface) but without any major contributions on the outermost atomic layers. At the same time, the energy of this state only slightly increases in passing from the LDA to the sc-PPA approach: from 0.22 to 0.42 eV above the Fermi energy (see Table I). In other words, the account of dynamic correlation “squeezes out” the inner slab contributions to the wave function and pushes the level at a slightly higher energy. One therefore faces a hybrid state which in terms of spatial localization has features similar to an image state but which—in contrast to typical image states—lies very close to the Fermi level instead of being close to the vacuum level. Such a hybrid state is clearly very difficult

to capture using model approaches.¹⁹ Similarly, the second excited state which from LDA comes out as a combination of a resonance and an image state becomes the second image state in the sc-PPA approach. It should be underlined that image states at the surface of ionic solids exist,^{10,25} but polarization screening and image charge effects are much weaker for a bulk dielectric, and such image states are extremely diffuse once dynamic correlation is accounted for,¹⁰ whereas in our case the underlying metal support crucially enhances image screening effects and keeps the image states much closer to the surface. In passing, it can be noted that correlation substantially modifies also the third excited state, transforming a particle-in-the-box level into an imagelike state (see Fig. 3).

When a second LiF ML is adsorbed on the LiF/Li(110) system to give a LiF BL, the situation changes once again. Now the first excited state definitely loses its component onto the surface top layers already at the LDA level (see Fig. 3). However, its low energy (see Table I) confirms that some resonance characteristics are still present, although the energy increase due to self-consistent GW effects is larger than in the ML case: from around 0.02 to 0.81 eV. The confinement effect due to the growing ultrathin dielectric overlayer thus progressively compresses the resonance wave function until it

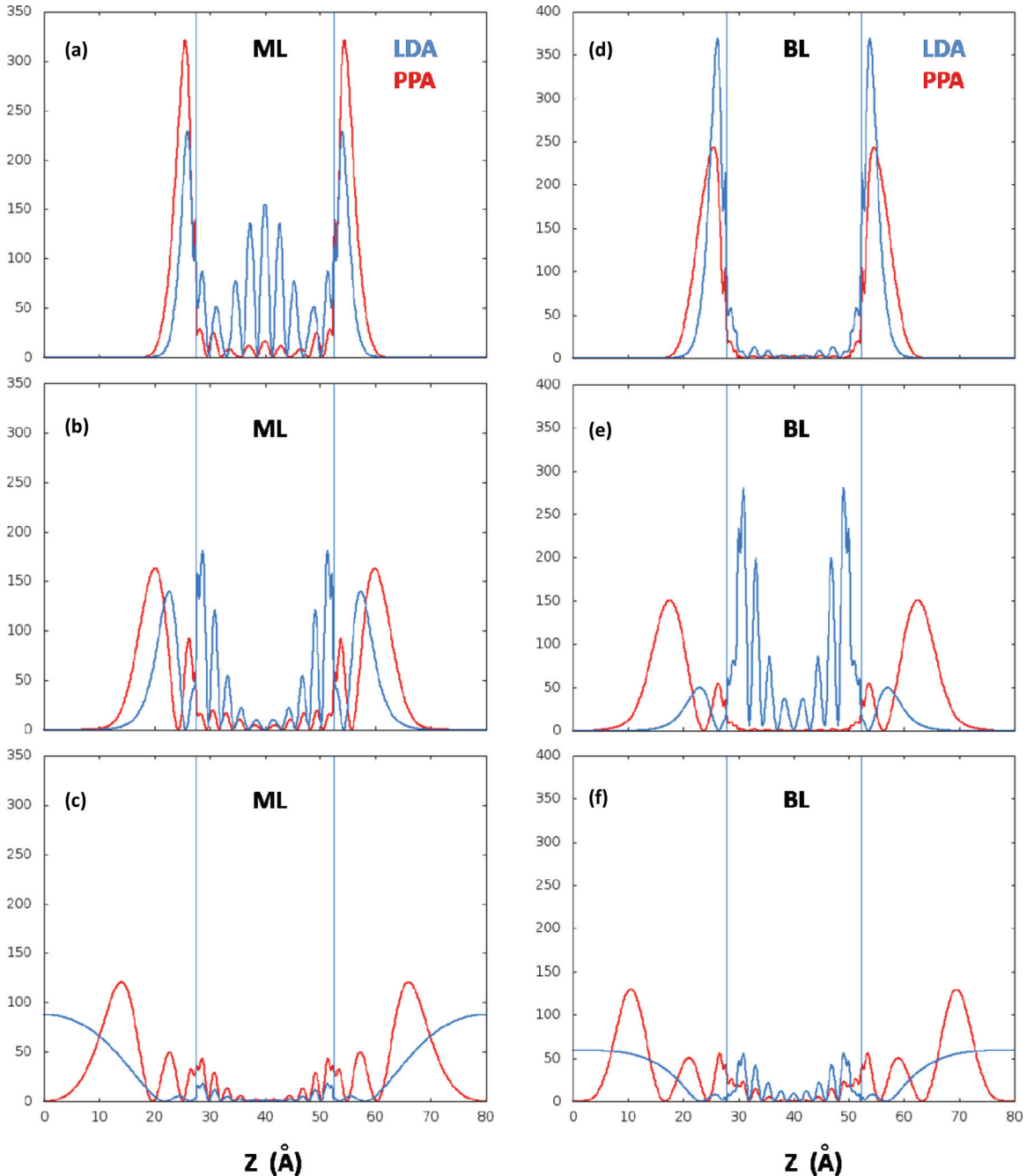


FIG. 3. (Color online) One-dimensional profiles along the z direction obtained by averaging over (x,y) planes the square modulus of the wave function for several excited states of (a)–(c) LiF(ML)/Li(110) and (d)–(f) LiF(BL)/Li(110) at the LDA [light gray (blue)] and QSGW-PPA [dark gray (red)] levels. The plots refer to the first (a), (d), second (b), (e), and third (c), (f) excited states. Z values in Å. The vertical lines indicate the position of the outmost surface layers.

eventually disappears and does not contribute any more to the electronic structure of the interface for thick LiF films (results not shown).

It is important to observe that the present results can be straightforwardly connected with STS observations of field emission resonances (FER),⁶ i.e., electronic excited states in the sample-tip electric field. In fact at zeroth order the effect of the field on the energy levels can be simply estimated by calculating the values of the average distance of the n th image states from the surface $\langle z_n \rangle$ (see the Supplemental Material¹³

for more details), a quantity which can be derived from sc-PPA wave functions and connected to the parameters in the experimental fitting of FER (a rigorous QSGW calculation including the effect of the electric field is in principle also possible). The energy values reported in Table I [together with the highly nonlinear behavior of the $\langle z_n \rangle$ values in Table S3 (Ref. 13)] show that not only the spatial profile (as apparent from Figs. 2 and 3) but also the energetic series of the system excited states do not exhibit a simple hydrogenic behavior, and cannot thus be reproduced in terms of standard parametric fits

TABLE I. Band and quasiparticle energies of selected levels at the Gamma point for the systems here investigated: pure metal slab [Li(110)] covered with a ML [LiF(ML)/Li(110)] or BL [LiF(BL)/Li(110)] LiF film. The Fermi level is taken as zero. All energies in eV.

Li(110)	LDA	PPA
Bulk	From -3.45 to -0.01	From -3.21 to -0.02
Surface resonance	+0.7	+1.2
Image state 1	+3.1	+3.0
Image state 2	+3.5	+3.6
LiF(ML)/Li(110)		
Bulk	From -3.47 to -0.22	From -3.75 to -0.60
First excited	+0.2	+0.4
Second excited	+1.4	+1.1
Third excited	+1.7	+1.6
LiF(BL)/Li(110)		
Bulk	From -3.21 to -0.32	From -3.52 to -0.47
First excited	+0.02	+0.8
Second excited	+1.2	+1.7
Third excited	+1.4	+2.0

(see the Supplemental Material¹³ for more details). We argue that the presence of these “intruder states” is the reason why the results of FER or STS measurements if analyzed in terms of simplified models do not give proper values of the system work function,^{6,12,26} in addition to the technical difficulties in predicting this quantity.^{27,28} We also argue that precisely this disagreement with the value of, say, the work function derived from other experimental techniques can be taken as a strong indication of the presence of resonances.

In summary, thanks to advances in hardware and computational methods the prediction of electronic excited states at

complex interfacial systems described with atomistic detail via fully first-principles (post-DFT) approaches is beginning to be accessible.²⁰ This has been explored in the present work in the case of prototypical dielectric ultrathin films, for which knowledge of electronic properties and the associated physics is still in a rudimentary stage, despite the interest they generate in terms of both basic science and potential applications.¹⁻³ Such a level of sophistication is shown to be needed for a correct analysis and understanding of the relevant phenomena, as the presence of surface states (here resonances but similar effects are expected, e.g., for Shockley states) and their coupling with image states can strongly perturb hydrogenic series and undermine the basis of both modellistic analyses^{6,12} and empirical corrections.¹⁹ Indeed in the present case it is found that the subtle interplay of interfacial and long-range character as a function of the charge compression²⁹ brought about by the growing ultrathin dielectric overlayer produces exotic low-energy electronic excited states with a hybrid localized but low-lying character. Accounting for the complex interactions leading to such peculiar states seems decisive, e.g., when interpreting experimental data on FER via STS⁶—once coupled with an external electric field—and in general in the study of electron relaxation and transport processes at such nanostructured interfaces, something which can hardly be achieved using simplified models which neglect the precise atomistic structure of the system.

Luca Gavioli, Gaetano Granozzi, and Falko Netzer are gratefully acknowledged for many enlightening discussions and giving a strong stimulus to the present work. Financial support was provided by the ERC Advanced Grant SEPON. Part of the calculations were performed at CINECA within the IS CRA IMAGINE project.

*alessandro.fortunelli@cnr.it

¹J. Repp, G. Meyer, S. Paavilainen, F. E. Olsson, and M. Persson, *Science* **312**, 1196 (2006).

²S. Surnev, A. Fortunelli, and F. P. Netzer, *Chem. Rev.* **113**, 4314 (2013).

³G. Pacchioni and H.-J. Freund, *Chem. Rev.* **113**, 4035 (2012).

⁴E. Bertel, *Surf. Sci.* **331**, 1136 (1995).

⁵W. A. Hofer, A. S. Foster, and A. L. Shluger, *Rev. Mod. Phys.* **75**, 1287 (2003).

⁶N. Nilius, *Surf. Sci. Rep.* **64**, 595 (2009).

⁷M. Winter, E. V. Chulkov, and U. Höfer, *Phys. Rev. Lett.* **107**, 236801 (2011).

⁸C. Freysoldt, P. Rinke, and M. Scheffler, *Phys. Rev. Lett.* **103**, 056803 (2009).

⁹I. D. White, R. W. Godby, M. M. Rieger, and R. J. Needs, *Phys. Rev. Lett.* **80**, 4265 (1998).

¹⁰R. L. Heinisch, F. X. Bronold, and H. Fehske, *Phys. Rev. B* **83**, 195407 (2011).

¹¹F. Bruneval, N. Vast, and L. Reining, *Phys. Rev. B* **74**, 045102 (2006).

¹²B. Borca, S. Barja, M. Garnica, D. Sánchez-Portal, V. M. Silkin, E. V. Chulkov, C. F. Hermanns, J. J. Hinarejos, A. L. Vázquez de Parga, A. Arnau, P. M. Echenique, and R. Miranda, *Phys. Rev. Lett.* **105**, 219702 (2010).

¹³See Supplemental Material at <http://link.aps.org/supplemental/10.1103/PhysRevB.88.125413> for work function and charge density analysis of the Li(100) and LiF/Li(100) ML and BL systems, plot of LDA mean-field potential and first image states, and comparison between one-electron and three-electron pseudopotential models.

¹⁴X. Gonze, B. Amadon, P. M. Anglade, J. M. Beuken, F. Bottin, P. Boulanger, F. Bruneval, D. Caliste, R. Caracas, M. Coteo, T. Deutsch, L. Genovese, Ph. Ghosez, M. Giantomassi, S. Goedecker, D. R. Hamann, P. Hermet, F. Jollet, G. Jomard, S. Leroux *et al.*, *Comput. Phys. Commun.* **180**, 2582 (2009).

¹⁵N. Troullier and J. L. Martins, *Phys. Rev. B* **43**, 1993 (1991).

¹⁶G. Fratesi, G. P. Brivio, P. Rinke, and R. W. Godby, *Phys. Rev. B* **68**, 195404 (2003).

¹⁷J. J. Deisz, A. G. Eguiluz, and W. Hanke, *Phys. Rev. Lett.* **71**, 2793 (1993).

¹⁸G. Onida, L. Reining, and A. Rubio, *Rev. Mod. Phys.* **74**, 601 (2002).

¹⁹E. V. Chulkov, V. M. Silkin, and P. M. Echenique, *Surf. Sci.* **437**, 330 (1999).

²⁰M. Giantomassi, M. Stankovski, R. Shaltaf, M. Grüning, F. Bruneval, P. Rinke, and G. M. Rignanese, *Phys. Status Solidi B* **248**, 275 (2011).

- ²¹F. Aryasetiawan and O. Gunnarsson, *Rep. Prog. Phys.* **61**, 237 (1998).
- ²²S. V. Faleev, M. van Schilfgaarde, and T. Kotani, *Phys. Rev. Lett.* **93**, 126406 (2004).
- ²³L. Hedin, *Phys. Rev.* **139**, A796 (1965).
- ²⁴R. W. Godby and R. J. Needs, *Phys. Rev. Lett.* **62**, 1169 (1989).
- ²⁵N. Rohlfing, in *High Performance Computing in Science and Engineering '04*, edited by E. Krause, W. Jage, and M. Resch (Springer, Berlin, 2004), pp. 57–66.
- ²⁶H. C. Ploigt, C. Brune, M. Pivetta, F. Patthey, and W. D. Schneider, *Phys. Rev. B* **76**, 195404 (2007).
- ²⁷I. Tamblyn, P. Darancet, S. Y. Quek, S. A. Bonev, and J. B. Neaton, *Phys. Rev. B* **84**, 201402 (2011).
- ²⁸S. V. Faleev, O. N. Mryasov, and T. R. Mattsson, *Phys. Rev. B* **81**, 205436 (2010).
- ²⁹L. Sementa, G. Barcaro, F. R. Negreiros, I. O. Thomas, F. P. Netzer, A. M. Ferrari, and A. Fortunelli, *J. Chem. Theory Comput.* **8**, 629 (2012).